Journal of Power Sources 303 (2016) 73–80

Contents lists available at ScienceDirect

Journal of Power Sources

journal homepage: www.elsevier.com/locate/jpowsour

A new generation of electrochemical supercapacitors based on layer-by-layer polymer films

Wania Ap. Christinelli, Roger Gonçalves, Ernesto C. Pereira*

Chemistry Dept., Federal University of São Carlos, C.P. 676, 13560-970 São Carlos, SP, Brazil

HIGHLIGHTS

- A new layer-by-layer conducting polymer is used as electrode.
- An important in the specific capacitance is observed.
- The results are explained by a self-doping effect in the layer-by-layer film.

GRAPHICAL ABSTRACT

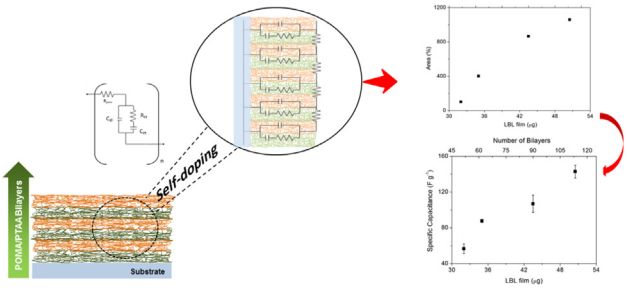

ARTICLE INFO

Article history:
Received 23 July 2015
Received in revised form
28 September 2015
Accepted 23 October 2015
Available online 8 November 2015

Keywords:
Conducting polymers
Supercapacitors
Layer-by-layer films
Self-doping

ABSTRACT

Here we report supercapacitors fabricated with the layer-by-layer (LBL) technique using two polymers, namely poly(o-methoxyaniline) (POMA) and poly(3-thiophene acetic acid) (PTAA). The electrochemical performances of POMA/PTAA supercapacitors were characterized by cyclic voltammetry and electrochemical impedance spectroscopy. The results were compared with POMA *casting* film. The specific capacitance of LBL films increases almost linearly with a number of bilayers which were not observed for POMA *casting* films. The results of this investigation demonstrate that the self-doping effect between POMA and PTAA can change the properties on films and can be successfully used as a supercapacitor technology.

1. Introduction

Research on new sources of energy conversion and storage is an issue that currently is an important need for the development of society. The synthesis of new materials for the production of modern devices enabling solutions for the world's energy problem has been the subject of intense research. This interest is not only related to the shortage of energy, but also new energy sources with low or even an absence of environmental impact. Considering the concerns mentioned, supercapacitors are promising devices [1–10]. Based on an energy storage mechanism, supercapacitors can be classified into two groups, electrochemical double layer capacitors (EDLC) and pseudocapacitors. To build a supercapacitor electrode, there are many factors which must be considered: surface area, electronic and ionic conductivity, and mechanical/chemical stability [11,12]. In particular, pseudocapacitors store charges by fast and reversible redox reactions. These devices are becoming an attractive research area because of their higher power density once they provide higher capacitance per gram than EDLCs devices [13,14]. As

* Corresponding author.
E-mail addresses: waniaac@gmail.com (W.Ap. Christinelli), roger.gabiru@gmail.com (R. Gonçalves), ernesto@ufscar.br (E.C. Pereira).

http://dx.doi.org/10.1016/j.jpowsour.2015.10.077
0378-7753/

proposed in a recent review [15], conducting polymers are interesting materials to use in supercapacitors, as they are characterized by high specific capacitance, low environmental impact, and high cycle stability [16]. In this application, it is important to stress that the polymers are cycled between reduced and oxidized phases during the discharge/charge procedures. Therefore, the kinetics of the redox process, which in this case involves also an ion intercalation (deintercalation) step to counterbalance the charge generated during the oxidation (reduction), must be studied and optimized once this is generally described as the slow step in the redox process [17]. One option to optimize this last process is the use of materials that present a self-doping effect [2,18–20] and, then, the neutralization of the charges generated is performed by self-doping itself. In most papers, self-doping is reached by the introduction of SO_3^- lateral groups in the polymeric chain [18,21]. In this case, consequently, the intercalation is at least partially inhibited. In a different approach to decrease the importance of the intercalation is the use of layer-by-layer (LBL) film to provide the self-doping effect in conducting polymers [22–26], and in this case, the self-doping effect occurs between two successive layers. In this sense, the present work investigates the specific capacitance of the LBL films of poly(o-methoxyaniline)/poly(3-thiopheneacetic acid) [POMA/PTAA], as electrochemical supercapacitors and compare it with those built using POMA *casting* films. It is important to stress that, in the present work, the only role of the PTAA layer is to provide the counter ion balance to the positive charge generated in the POMA chains. This occurs due to the carboxylic groups in the thiopheneacetic acid monomer, which can easily be deprotonated and could have a strong interaction with the amine/imine group in aniline monomers by both H-bond and/or electrostatic interaction.

2. Experimental

2.1. Materials and methods

All the reactants were supplied by Sigma–Aldrich, the anisidine monomer was used after distillation process and the 3-thiophene acetic acid monomer was uses without previous purification. Analytical grade lithium perchlorate and acetonitrile were used for the electrochemical characterizations.

The layer-by-layer films were assembled using a homemade robot developed specifically for this task [27]. The polycation solution of POMA was prepared by dissolving the polymer in a mixture of H_2O and acetonitrile (ACN) in a proportion of 59:1 (v/v), the use of ACN are to enhance the solubility of the polymer in water. The polyanion solution, PTAA, was prepared by dissolving PTAA in 0.1 M NH_4OH solution, with the final pH being adjusted to 8 by the addition of 0.1 M HCl solution [28]. Both solutions were centrifuged using EPPENDORF centrifuge 5804, and the insoluble residues were discarded. POMA and PTAA has been synthesized by chemical direct oxidation of the monomer as described by MacDiarmind [18] and Sugimoto [29], respectively. Glass substrates covered with indium tin oxide (ITO) (Geometrical area = 1 cm^2) was used as substrate for the working electrodes. These substrates were previously etched with a $H_2O_2/NH_4OH/H_2O$ [1:1:5 (v/v)] solution and ultrapure water (Milli-Q system) to prepare a hydrophilic surface. Thus, the first monolayer was assembled by immersing the substrate in the POMA polycation solution for 180 s. Then, the substrate was immersed in the PTAA polyanion solution for 180 s. Between each of those steps, the films were washed in water with pH adjusted to the same value as the deposition solution and then dried in N_2 flux for 100 s. These steps were repeated until the desired number of layers was reached. Fig.1 presents a schematic representation of experimental buildup of self-assembled films.

In order to compare the results with conventional conducting polymer films, it used POMA electrodes prepared by *casting* from the POMA solution on the ITO substrate. Films containing different masses by both techniques, LBL and *casting*, were built and they have been characterized by different methods.

2.2. Characterizations

The growth of the films prepared by both methods, LBL and *casting*, were followed by visible spectroscopy using UV–VIS–NIR spectrophotometer (Cary model 5G) and by mass measurements. Its morphology was measured by Atomic Force Microscopy (AFM), using a 2100 SPM microscope (molecular imaging) model Pico LE™. Electrochemical experiments were carried out in a three-electrode glass cell using an EG&G PARC 273 potentiostat. The measurements were performed in an acetonitrile solution with 0.1 M $LiClO_4$. As a reference to auxiliary electrodes, an Ag pseudo-reference electrode and Pt sheet (area 1 cm^2) were used, respectively. The electrochemical performance was carried out using voltammetry cyclic and electrochemical impedance spectroscopy techniques. All experiments were carried out at room temperature. Cyclic voltammetry (CV) was carried out at a scan rate of 20 mV s^{-1} from −0.3–0.5 V versus Ag. The measurements of electrochemical impedance spectroscopy (EIS) were carried out at 0.3 V, frequency range from 10 kHz to 10 mHz with an applied ac potential of 0.01 V. The specific capacitances were calculated by the CVs using the method proposed by Ramya [16] and Zhao [30].

3. Results and discussions

The growth of the POMA *casting* and LBL POMA/PTAA films was monitored by UV–VIS absorption after the deposition process. Fig. 2a presents the UV–VIS absorption spectra of the POMA *casting* films on the ITO substrate. There is an increase in the absorption between absorbance and the POMA mass deposited on the substrate. The behavior is quantitatively reproducible. The POMA spectra exhibit a typical absorption peak around 450 nm, (Insert of Fig. 2a), in agreement with the literature [26,31].

The mass measurement of POMA *casting* films is shown in Fig. 2b. The nearly linear increase of mass with POMA indicates that the buildup of film is reproducible. The active mass considered was the total mass shown in Fig. 2b.

Scanning Atomic Force Microscopy (AFM) images were recorded over a scan area from 0.3 × 0.3 μm with a scan rate of 1 line s^{-1}, Fig. 2c, were used for determination of morphology of films. The AFM images show a complete cover of the polymeric material over the substrate, and that film has the typical globular topography also in agreement with literature [32–34].

To compare these data, Fig. 3a shows UV–VIS absorption spectra of POMA/PTAA LBL films on the ITO substrate. The increase of absorbance as an increase in the number of bilayer absorbance indicates that the deposition is reproducible from one layer to another. The POMA/PTAA exhibit a typical absorption peak at around 450 nm (Insert of Fig. 3a), as observed for POMA *casting* films. The mass measurement of LBL films was shown in Fig.3b. The nearly linear increase of mass with the number of bilayers indicates that the amount of polymers adsorbed in each bilayer are the same. The active mass considered was a half value of the total mass showed in Fig. 3b. This consideration can be made because only POMA is electroactive in the potential window used. Furthermore, the polymeric adsorption and total mass on LBL films increases linearly the number of bilayer increases, as described above. Comparing those results presented in Figs. 2 and 3, it is important to stress out that the higher mass of the LBL films could be attributed to the presence of the PTAA layers in the material.

Finally, AFM, Fig. 3c, show that film has the typical globular

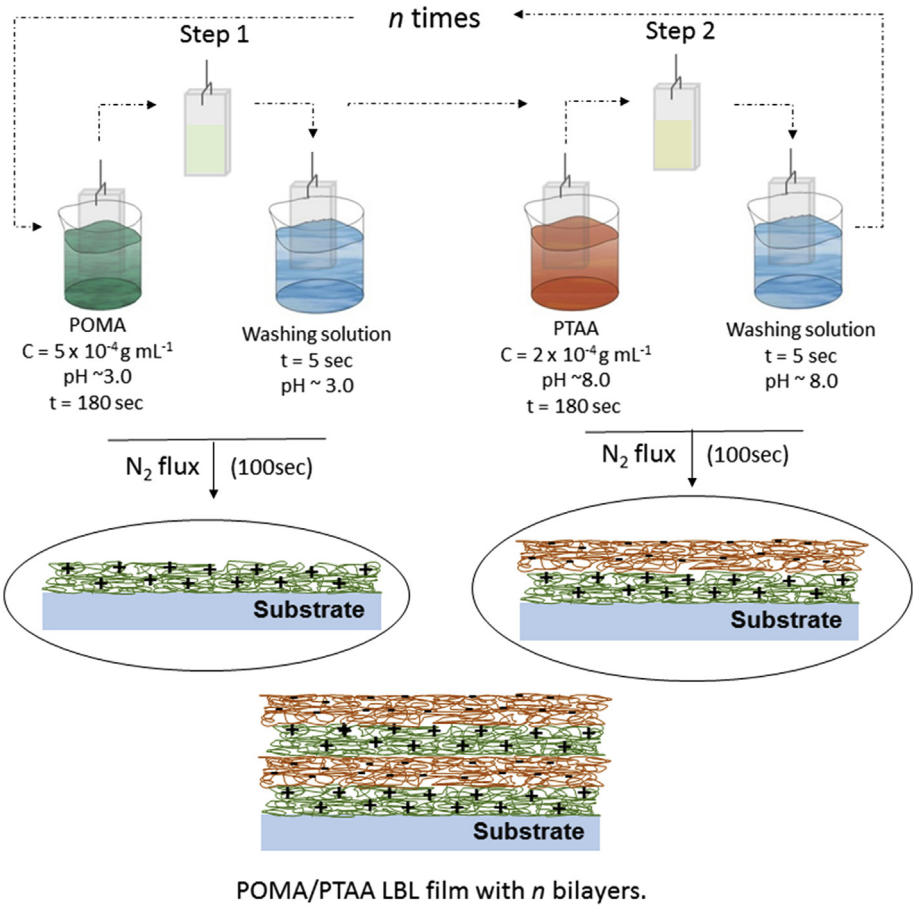

Fig. 1. Schematic representation of the buildup of a self-assembled film.

topography as the same one observed in POMA *casting* films, but with larger globules.

The electrochemical characterization was carried out using cyclic voltammetry and impedance spectroscopy. The first one is useful to characterize the electrochemical redox process as well their reversibility and stability. Fig. 4 presents the cyclic voltammograms (CV) for both materials, POMA *casting* and POMA/PTAA LBL, in ACN with 0.1 mol L^{-1} $LiClO_4$ as supporting electrolyte. It is possible to observe that voltammograms POMA *casting*, and POMA/PTAA LBL films, each have a similar profile. This is an expected result once POMA is the only electroactive material in both samples. In this sense, in the potential window from −0.3 V to 0.3 V, where it is the first redox pairing of POMA [18], which corresponds to the oxidation of leucoesmeraldine to esmeraldine, during the sweep towards more positive potentials, and the reverse process during the cathodic sweep. An important difference observed in Fig. 4 is an increase in the normalized current by the sample mass for the POMA/PTAA LBL, which means that the electroactivity of this sample is superior to that of the POMA *casting* film. Although we do not have a complete proposition to explain this result, one possible explanation is the self-doping effect which occurs in an LBL sample [25]. In conducting polymers, the oxidation (reduction) leads to the intercalation of counter ions (deintercalation) to compensate for the generated charge in the material. When a self-doping effect occurs [25,35–37], the ion transport is partially (or totally) inhibited and, as consequence, an increase in efficiency of the electrochemical process can be expected. In the present case, there is an increase of the anodic current/mass up to 3.5 times. There is a second important observation comparing Fig. 4a (POMA *casting*) and Fig. 4c (POMA/PTAA LBL). For the thinnest films, the current/mass are equal, whereas thick films increase this parameter, also increasing the LBL film present I/m values 3.5 times higher than *casting* one. As a consequence, the specific capacitance values calculated from the voltammetric curves present the same kind of behavior, although the values calculated for the *casting* film remains constant near 60 F g^{-1}, the LBL film almost linearly increases from 50 F g^{-1} up to 140 F g^{-1}. Of course, this is an unexpected result. Besides, the increase of the specific capacitance for the LBL film has many important applications in the development of different electrochemical devices. In order to further understand these interesting behaviors, we carried out electrochemical impedance measurements.

Fig. 5 shows the Nyquist plots as well as their fitted values and circuit used to fit the results. Considering those models proposed in the literature to analyze impedance data of porous polymeric materials [38,39], we have to use a transmission line model to interpret the data. A conventional equivalent circuit cannot be used to interpret the data of porous media where there is an electric potential drop along the pores. The existence of this potential drop can characterize the change in behavior from a rough material to a porous one. The use of transmission line model for porous materials, is adequate because, in our opinion, any intercalation material is a porous materials from an electrochemical point of view [40,41].

Besides, in the present case we detected the need to use to two different models to analyze the data obtained from *casting* (Fig. 5a) and LBL films (Fig. 5b). In the first case, *casting* POMA films, the repetitive unit, which repeats throughout the interface pore/solution, was built up using resistences to describe ionic charge

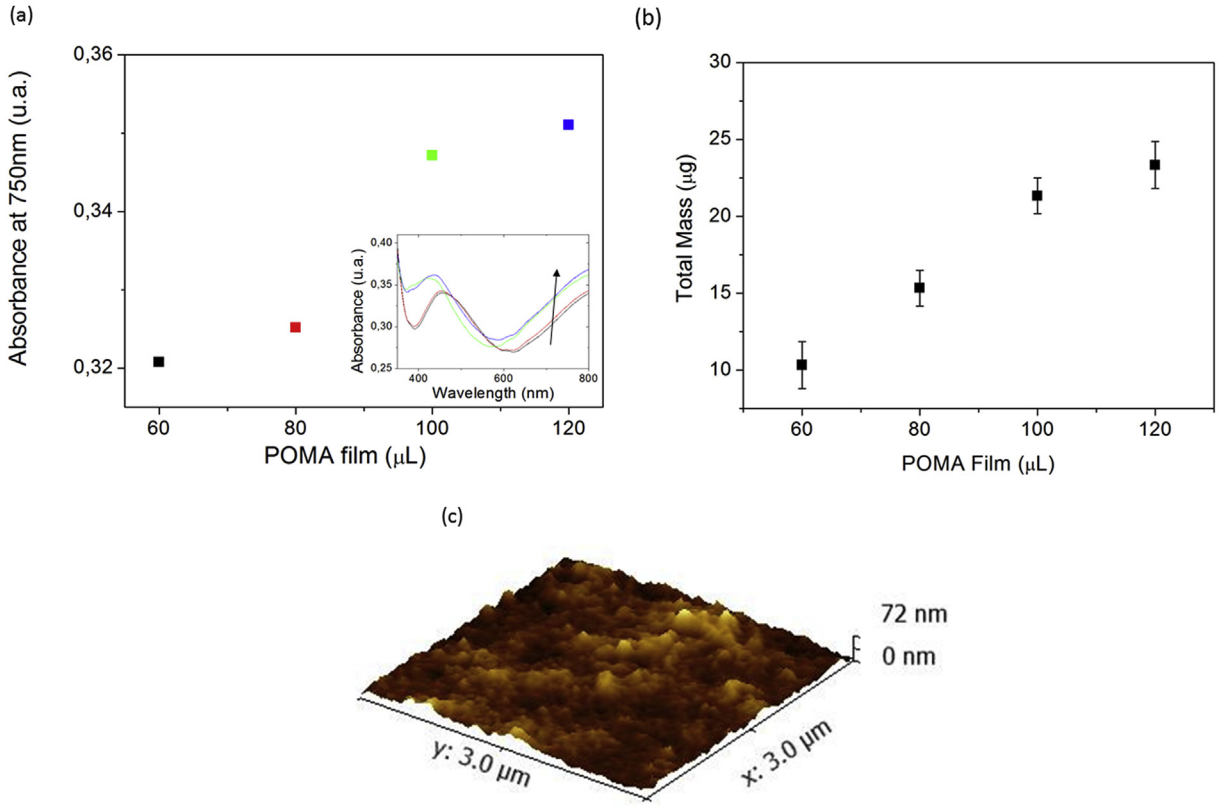

Fig. 2. (a) Plot of absorbance at 750 nm vs. POMA films (μL). The insert is a UV–VIS absorption spectra of POMA *casting* films on ITO substrate. (b) Total mass of the films vs. POMA volume solution. (c) Tapping Mode AFM Topography images of POMA *casting* films.

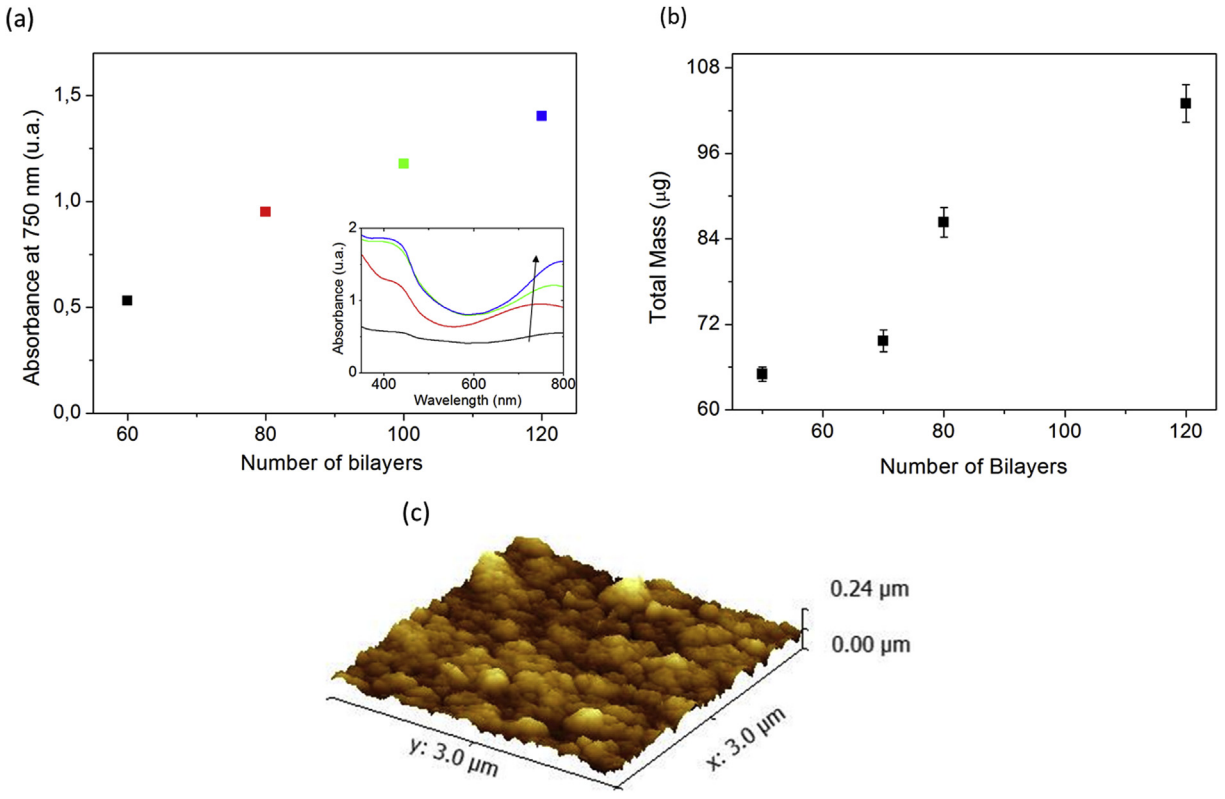

Fig. 3. (a) Plot of absorbance at 750 nm vs. number of bilayers of POMA/PTAA films. The insert is a UV–VIS absorption spectra of POMA/PTAA LBL film on ITO substrate. (b) Total mass vs. number of bilayers of POMA/PTAA LBL film. (c) Tapping Mode AFM Topography images of POMA/PTAA LBL films.

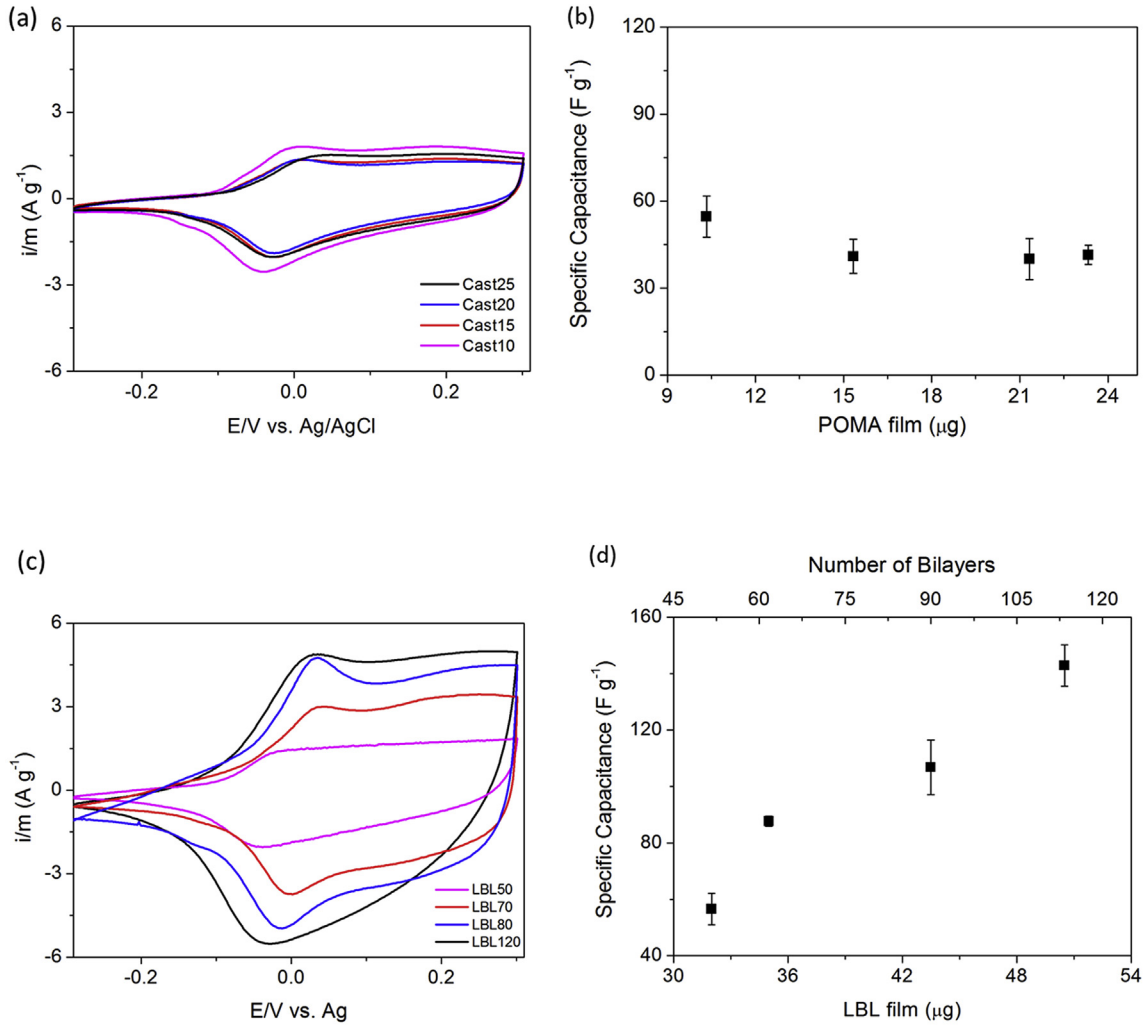

Fig. 4. Cyclic voltammogram for (a) POMA *casting* and (c) POMA/PTAA LBL films, (b) Specific capacitance for (a) POMA *casting* and (c) POMA/PTAA LBL films at different POMA film (μL) and number of bilayers, respectively. Measurements were made in ACN at 20 mV s^{-1}.

transports inside the pores (Rpore). The use of only a resistence (Rpol) to describe the polymer chain can be expected; in this case, the polymer is conductive state, because of potential value whereupon the impedance data were collected (E = 0.3 V *vs* Ag wire). Generally, in bulk solution with supporting electrolyte, the ionic transport is described by a Warburg element. However, the situation could be completely different inside the pores due to their limited size, existence of several kinds of traps and the non-equilibrium condition between those ions inside and in the bulk of the solution. Then, the need to use only a resistance to describe process could be explained by the ionic transport in the solution pores to be of a migratory kind. In the other hand, the interface between the polymeric chains and the solution in both cases, *casting* and LBL films, has been described by a modified double layer capacitance, Cdl, and charge transfer resistance, Rct, in parallel. In addition, as well in different papers in the literature [38,39], there is the need to add a second capacitance (Cct) in series with the Rct element. This second pseudocapacitance is related to the fact that the transported charged species across the interface are ions (during the intercalation/deintercalation process). Then, in a different manner from an electronic (hole) defect, the mass of ions can have an important role in the process. We propose that after its intercalation, there is a delay until these ions couple to a charge trap in the polymeric chain, generating a charge separation and, as a consequence, a charge storage process, leading addition need of this element in the model that fits the data in all the frequency range.

There is, otherwise, a difference in the models to describe the *casting* POMA film and the POMA/PTAA LBL material. For the LBL film (Fig. 5b), there is no need to describe the polymer resistance; in other words, its values are negligible compared to the dissipative process in the pores. One possible explanation for this fact is related to the self-doping effect. As described in a different paper, the POMA/PTAA LBL films present a self-doping effect and, as consequence, there is no need, at least partially, of ion transport in the polymer to compensate the charge. Then, each bilayer can act as a full independent polymer unit with (at least partially) no need to intercalate (or deintercalate) ions during electrochemical oxidation (reduction). If this is the case, as suggested by the model which describes the LBL films, there is no ohmic drop along with the film thickness, and then its resistance is negligible. A schematic representation of the "new" material configuration is presented in Fig. 6 as well as for the POMA *casting* film.

In this schematic representation, it is described how LBL films behave with increasing of bilayers number; We understand this behave that it is as if each bilayer was connected shorted to the substrate and for this reason there is no resistance associated with the polymer branch. Causing the capacitance specifies each layer to

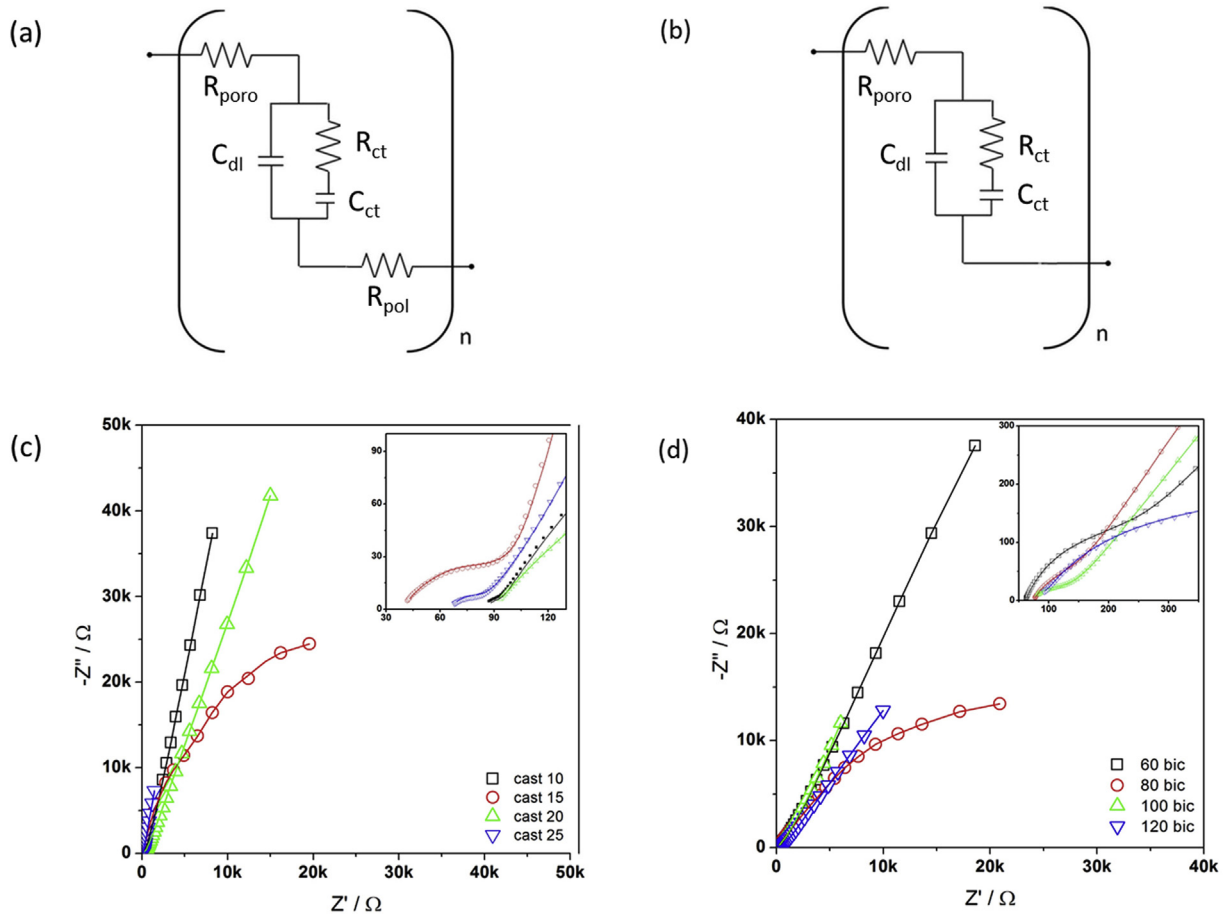

Fig. 5. Schematic presentation of the models proposed for (a) POMA *casting* and (b) POMA/PTAA films. Nyquist diagrams for (c) POMA *casting* and (d) POMA/PTAA films. The data were collected in ACN solution with 0.1 M $LiClO_4$ as supporting electrolyte at room temperature.

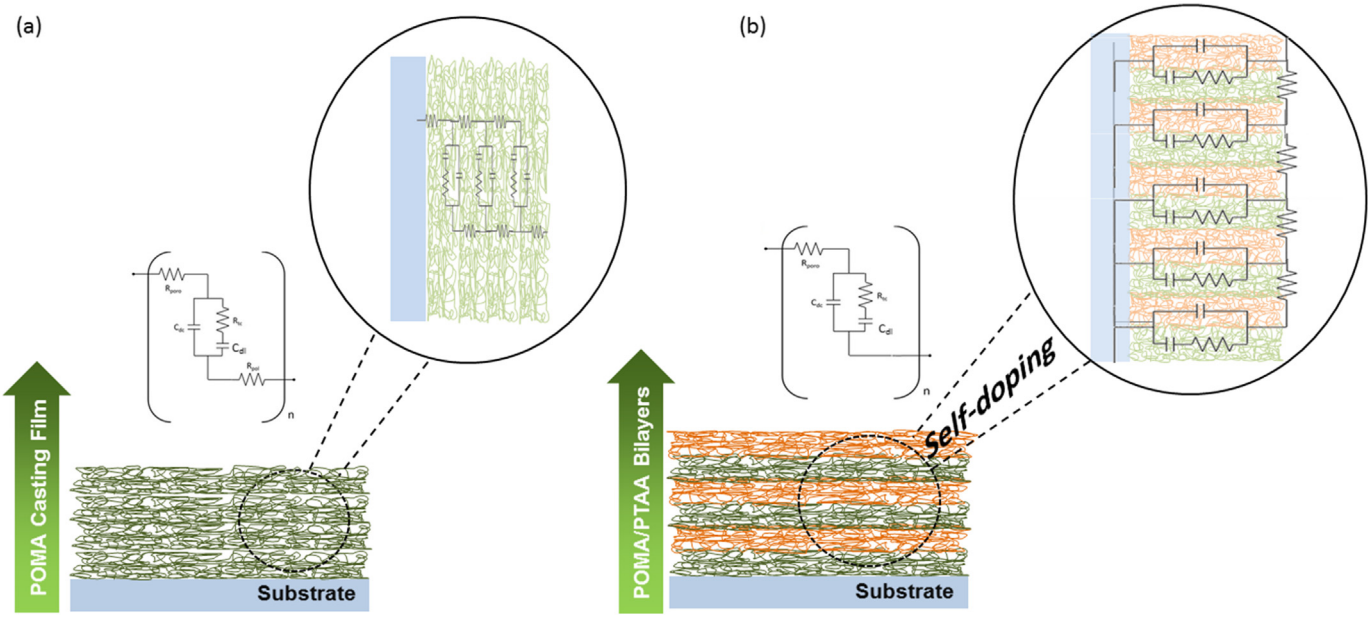

Fig. 6. Schematic representation for (a) POMA *casting* films and (b) POMA/PTAA LBL films.

behave like capacitors in parallel, increasing the overall capacitance of the film, as it was an area increase. Therefore, in this proposition, is reasonable to expect that the film active area increase as the number of bilayers increase. Then, in Fig. 7, it is presented the

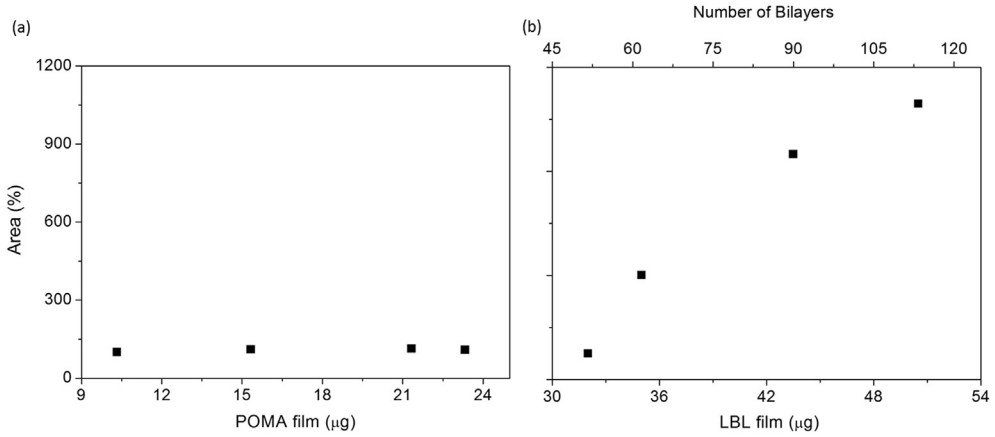

Fig. 7. Area Change for (a) POMA *casting* and (b) POMA/PTAA LBL films calculated from the double layer capacitance of impedance results.

normalized area change calculated from the impedance data, specifically from the double layer capacitance. The only hypotheses need for this calculation is that each bilayer is equivalent and there is no change in the charge storage efficiency among them; i.e, each bilayer stores the same amount of charge.

As expected, there is a linear relationship between the specific capacitance, calculated from the voltammetric data and the area change calculated from the impedance one, Fig. 7b in the case of an LBL system. Then, one possible explanation for the most impressive results are described; i.e., an increase specific capacitance as the number of bilayers in a POMA/PTAA LBL film is increased could be explained by the autodoping effect observed in this system, which leads to each bilayers acting as independent material as the counter ion intercalation process is inhibited. A proof of this proposition is the need for a change in the model used to describe the impedance results. For the LBL film, there is no need to describe the potential drop inside the polymer chains, and as consequence, material setup over the electrode could be described in a different form (presented in Fig. 6). A further support to these ideas is the change to the double layer area, which was calculated from the double layer capacitance, which also increases linearly as the number of bilayers increases.

4. Conclusions

In summary, in this work, it was an LBL film was prepared, which had main characteristics of increasing the redox process efficiency as well as an increase in the specific capacitance as the number of bilayers increase. Using a transmission line model to modeling the impedance data, it was observed that polymer resistance is negligible. This behavior is equivalent to propose the existence of a short circuit between the bilayers or, different, that each bilayer acts if it is in direct contact with the electrical contact. A possible explanation for this fact is the inhibition of the ionic charge intercalation promoted by the interaction between the carboxylate group in the PTAA unit and the amine one in the POMA layer.

Acknowledgments

The support of this research by FAPESP (Grant# 2011/10897-2, 2013/07296-2), CAPES, and CNPq is gratefully acknowledged.

References

[1] C. Arbizzani, M. Mastragostino, L. Meneghello, Polymer-based redox supercapacitors: a comparative study, Electrochim. Acta 41 (1996) 21–26, http://dx.doi.org/10.1016/0013-4686(95)00289-Q.
[2] R. Kötz, R. Kötz, M. Carlen, M. Carlen, Principles and applications of electrochemical capacitors, Electrochim. Acta 45 (2000) 2483–2498, http://dx.doi.org/10.1016/S0013-4686(00)00354-6.
[3] M. Mastragostino, C. Arbizzani, F. Soavi, Polymer-based supercapacitors, J. Power Sources 97–98 (2001) 812–815, http://dx.doi.org/10.1016/S0378-7753(01)00613-9.
[4] C. Arbizzani, M. Mastragostino, F. Soavi, New trends in electrochemical supercapacitors, J. Power Sources 100 (2001) 164–170, http://dx.doi.org/10.1016/S0378-7753(01)00892-8.
[5] C. Yang, H. Wei, L. Guan, J. Guo, Y. Wang, X. Yan, et al., Polymer nanocomposites for energy storage, energy saving, and anticorrosion, J. Mater. Chem. A 3 (2015) 14929–14941, http://dx.doi.org/10.1039/C5TA02707A.
[6] H. Wei, C. He, J. Liu, H. Gu, Y. Wang, X. Yan, et al., Electropolymerized polypyrrole nanocomposites with cobalt oxide coated on carbon paper for electrochemical energy storage, Polym. Guildf. 67 (2015) 192–199, http://dx.doi.org/10.1016/j.polymer.2015.04.064.
[7] Huige Wei, Hongbo Gu, Jiang Guo, Suying Wei, Zhanhu Guo, Electropolymerized polyaniline nanocomposites from multi-walled carbon nanotubes with tuned surface functionalities for electrochemical energy storage, J. Electrochem. Soc. 160 (2013) G3038–G3045.
[8] H. Gu, H. Wei, J. Guo, N. Haldolaarachige, D.P. Young, S. Wei, et al., Hexavalent chromium synthesized polyaniline nanostructures: magnetoresistance and electrochemical energy storage behaviors, Polym. (United Kingdom) 54 (2013) 5974–5985, http://dx.doi.org/10.1016/j.polymer.2013.08.020.
[9] H. Wei, Y. Wang, J. Guo, X. Yan, R. O'Connor, X. Zhang, et al., Electropolymerized polypyrrole nanocoatings on carbon paper for electrochemical energy storage, ChemElectroChem. 2 (2015) 119–126, http://dx.doi.org/10.1002/celc.201402258.
[10] Z. Guo, Y. Wang, H. Wei, J. Liu, J. Wang, J. Guo, et al., Electropolymerized polyaniline/manganese iron oxide hybrids with enhanced color switching response and electrochemical energy storage, J. Mater. Chem. A (2015), http://dx.doi.org/10.1039/C5TA04439A.
[11] M. Halper, J. Ellenbogen, Supercapacitors: a Brief Overview, The Mitre Corporation, Virginia, USA, 2006.
[12] Z. Yu, L. Tetard, L. Zhai, J. Thomas, Supercapacitor electrode materials: nanostructures from 0 to 3 dimensions, Energy Environ. Sci. 8 (2014) 702–730, http://dx.doi.org/10.1039/C4EE03229B.
[13] Y. Sun, Q. Wu, G. Shi, Supercapacitors based on self-assembled graphene organogel. Phys. Chem. Chem. Phys. 13 (2011) 17249–17254, http://dx.doi.org/10.1039/c1cp22409c.
[14] G. Wang, L. Zhang, J. Zhang, A review of electrode materials for electrochemical supercapacitors. Chem. Soc. Rev. 41 (2012) 797–828, http://dx.doi.org/10.1039/c1cs15060j.
[15] G. Inzelt, Rise and rise of conducting polymers, J. Solid State Electrochem (2011), http://dx.doi.org/10.1007/s10008-011-1338-3.
[16] R. Ramya, R. Sivasubramanian, M.V. Sangaranarayanan, Conducting polymers-based electrochemical supercapacitors-progress and prospects, Electrochim. Acta 101 (2013) 109–129, http://dx.doi.org/10.1016/j.electacta.2012.09.116.
[17] J. Heinze, B.A. Frontana-Uribe, S. Ludwigs, Electrochemistry of conducting polymers–persistent models and new concepts. Chem. Rev. 110 (2010) 4724–4771, http://dx.doi.org/10.1021/cr900226k.
[18] L.H.C. Mattoso, A.G. MacDiarmid, A.J. Epstein, Controlled synthesis of high molecular weight polyaniline and poly(o-methoxyaniline), Synth. Met. 68 (1994) 1–11.
[19] M.A. Bavio, G.G. Acosta, T. Kessler, Synthesis and characterization of polyaniline and polyaniline – carbon nanotubes nanostructures for electrochemical supercapacitors, J. Power Sources 245 (2014) 475–481, http://dx.doi.org/10.1016/j.jpowsour.2013.06.119.
[20] A.K. Sarker, J.-D. Hong, Layer-by-layer self-assembled multi layer films

composed of graphene/polyaniline bilayers: high-energy electrode materials for supercapacitors, Langmuir 28 (2012) 12637–12646, http://dx.doi.org/10.1021/la3021589.
[21] A.G. MacDiarmid, A review of conductive polymer batteries, Abstr. Pap. Am. Chem. Soc. 186 (1983), 15–INDE.
[22] J.H. Cheung, A.F. Fou, M.F. Rubner, Molecular self-assembly of conducting, Polymers 244 (1994) 985–989.
[23] C.A. Constantine, S.V. Mello, A. Dupont, X.H. Cao, D. Santos, O.N. Oliveira, et al., Layer-by-layer self-assembled chitosan/poly(thiophene-3-acetic acid) and organophosphorus hydrolase multilayers, J. Am. Chem. Soc. 125 (2003) 1805–1809.
[24] F. Trivinho-Strixino, E.C. Pereira, S.V. Mello, O.N. Oliveira, Ions transport and self-doping in layer-by-layer conducting polymer films, Synth. Met. 155 (2005) 648–651, http://dx.doi.org/10.1016/j.synthmet.2005.08.021.
[25] F. Trivinho-Strixino, E.C. Pereira, S.V. Mello, O.N. Oliveira, Self-doping effect in poly(o-methoxyaniline)/poly(3-thiopheneacetic acid) layer-by-layer films. Langmuir 20 (2004) 3740–3745. http://www.ncbi.nlm.nih.gov/pubmed/15875409.
[26] S.V. Mello, E.C. Pereira, O.N. Oliveira, Poly(3-thiophene acetic acid) poly(o-methoxyaniline) self-assembled films, Synth. Met. 102 (1999) 1204.
[27] F. Trivinho-Strixino, E.C. Pereira, L.R.C. Lopes, Development of an automated device for fabrication of self-assembled films. Quim. Nova 27 (2004) 661–663.
[28] M. Giglioti, F. Trivinho-Strixino, J.T. Matsushima, L.O.S. Bulhoes, E.C. Pereira, Electrochemical and electrochromic response of poly(thiophene-3-acetic acid) films, Sol. Energy Mater. Sol. Cells 82 (2004) 413–420.
[29] K. Sugimoto, R. Taketa, S. Gu, H.B. Yoshino, Preparation of soluble polythiophene derivatives utilizing transition metal halides as catalysts and their property, Chem. Express 1 (1986) 635–638.
[30] Y. Zhao, H. Wei, M. Arowo, X. Yan, W. Wu, J. Chen, et al., Electrochemical energy storage by polyaniline nanofibers: high gravity assisted oxidative polymerization vs. rapid mixing chemical oxidative polymerization, Phys. Chem. Chem. Phys. 17 (2015) 1498–1502, http://dx.doi.org/10.1039/C4CP03144J.
[31] D. Goncalves, D.S. dosSantos, L.H.C. Mattoso, F.E. Karasz, L. Akcelrud, R.M. Faria, Poly(o-methoxyaniline): solubility, deprotonation-protonation process in solution and cast films, Synth. Met. 90 (1997) 5–11, http://dx.doi.org/10.1016/S0379-6779(97)03895-2.
[32] E. Frackowiak, V. Khomenko, K. Jurewicz, K. Lota, F. Béguin, Supercapacitors based on conducting polymers/nanotubes composites, J. Power Sources 153 (2006) 413–418, http://dx.doi.org/10.1016/j.jpowsour.2005.05.030.
[33] D.-H. Han, H.J. Lee, S.-M. Park, Electrochemistry of conductive polymers XXXV: electrical and morphological characteristics of polypyrrole films prepared in aqueous media studied by current sensing atomic force microscopy, Electrochim. Acta 50 (2005) 3085–3092, http://dx.doi.org/10.1016/j.electacta.2004.10.085.
[34] K. Bieńkowski, M. Strawski, M. Szklarczyk, The determination of the thickness of electrodeposited polymeric films by AFM and electrochemical techniques, J. Electroanal. Chem. 662 (2011) 196–203, http://dx.doi.org/10.1016/j.jelechem.2011.06.014.
[35] A. Malinauskas, Self-doped polyanilines, J. Power Sources 126 (2004) 214–220, http://dx.doi.org/10.1016/j.jpowsour.2003.08.008.
[36] B.A. Deore, M.S. Freund, Self-doped polyaniline nanoparticle dispersions based on boronic acid–phosphate complexation, Macromolecules 42 (2009) 164–168, http://dx.doi.org/10.1021/ma8020344.
[37] Z. Zhang, L. Wang, J. Deng, M. Wan, Self-assembled nanostructures of polyaniline doped with poly(3-thiopheneacetic acid), React. Funct. Polym. 68 (2008) 1081–1087, http://dx.doi.org/10.1016/j.reactfunctpolym.2008.02.010.
[38] L.F.Q.P. Marchesi, F.R. Simões, L.A. Pocrifka, E.C. Pereira, Investigation of polypyrrole degradation using electrochemical impedance spectroscopy. J. Phys. Chem. B 115 (2011) 9570–9575, http://dx.doi.org/10.1021/jp2041263.
[39] G. Garcia-Belmonte, J. Bisquert, E.C. Pereira, F. Fabregat-Santiago, Switching behaviour in lightly doped polymeric porous film electrodes. Improving distributed impedance models for mixed conduction conditions, J. Electroanal. Chem. 508 (2001) 48–58.
[40] G. Paasch, Complete electrochemical transmission line model for conducting polymers, Synth. Met. 119 (2001) 233–234, http://dx.doi.org/10.1016/S0379-6779(00)00865-1.
[41] G. Paasch, Transmission line description for doped conjugated polymers with polarons, bipolarons and counterions as charged species, Electrochim. Acta 47 (2002) 2049–2053, http://dx.doi.org/10.1016/S0013-4686(02)00072-5.